

The period-luminosity relation for type II Cepheids in globular clusters

Noriyuki Matsunaga^{1*}, Hinako Fukushi¹, Yoshikazu Nakada^{2,1}, Toshihiko Tanabé¹, Michael W. Feast³, John W. Menzies⁴, Yoshifusa Ita⁵, Shogo Nishiyama⁶, Daisuke Baba⁶, Takahiro Naoi⁵, Hidehiko Nakaya⁷, Takahiro Kawadu⁸, Akika Ishihara^{9,10} and Daisuke Kato⁶

¹ Institute of Astronomy, School of Science, the University of Tokyo, 2-21-1 Osawa, Mitaka, Tokyo 181-0015, Japan

² Kiso Observatory, Institute of Astronomy, School of Science, the University of Tokyo, Mitake, Kiso, Nagano 397-0101, Japan

³ Astronomy Department, University of Cape Town, 7701, Rondebosch, South Africa

⁴ South African Astronomical Observatory, PO Box 9, 7935, Observatory, South Africa

⁵ Institute of Space and Astronomical Science, Japan Aerospace Exploration Agency, Yoshinodai 3-1-1, Sagami-hara, Kanagawa 229-8510, Japan

⁶ Department of Astrophysics, Nagoya University, Furo-cho, Chikusa-ku, Nagoya 464-8602, Japan

⁷ Subaru Telescope, National Astronomical Observatory of Japan, 650 North Aohoku Place, Hilo, HI 96720, USA

⁸ Department of Astronomy, Kyoto University, Kitashirakawa-Oiwake-cho, Sakyo-ku, Kyoto 606-8502, Japan

⁹ National Astronomical Observatory of Japan, 2-21-1 Osawa, Mitaka, Tokyo 181-8588, Japan

¹⁰ Department of Earth and Planetary Science, School of Science, the University of Tokyo, 7-3-1 Hongo, Bunkyo-ku, Tokyo 113-0033, Japan

Accepted 2006 May 26. Received 2006 May 16; in original form 2006 March 30

ABSTRACT

We report the result of our near-infrared observations (JHK_s) for type II Cepheids (including possible RV Tau stars) in galactic globular clusters. We detected variations of 46 variables in 26 clusters (10 new discoveries in seven clusters) and present their light curves. Their periods range from 1.2 d to over 80 d. They show a well-defined period-luminosity relation at each wavelength. Two type II Cepheids in NGC 6441 also obey the relation if we assume the horizontal branch stars in NGC 6441 are as bright as those in metal-poor globular clusters in spite of the high metallicity of the cluster. This result supports the high luminosity which has been suggested for the RR Lyr variables in this cluster. The period-luminosity relation can be reproduced using the pulsation equation ($P\sqrt{\rho} = Q$) assuming that all the stars have the same mass. Cluster RR Lyr variables were found to lie on an extrapolation of the period-luminosity relation. These results provide important constraints on the parameters of the variable stars.

Using Two Micron All-Sky Survey (2MASS) data, we show that the type II Cepheids in the Large Magellanic Cloud (LMC) fit our period-luminosity relation within the expected scatter at the shorter periods. However, at long periods ($P > 40$ d, i.e. in the RV Tau star range) the LMC field variables are brighter by about one magnitude than those of similar periods in galactic globular clusters. The long-period cluster stars also differ from both these LMC stars and galactic field RV Tau stars in a colour-colour diagram. The reasons for these differences are discussed.

Key words: stars: Population II – stars: variables: other – globular clusters: general – infrared: stars.

1 INTRODUCTION

Type II Cepheids (hereafter T2Cs) are variables in the Cepheid instability strip, but belong to older populations than classical Cepheids. (see Wallerstein 2002, and references therein, for a review). They reside in globular clusters, the thick disc, the bulge

and the halo, but not in the thin disc or spiral arms. Based on their periods, they are often separated into BL Her stars ($P < 7$ d), W Vir stars ($7 < P < 20$ d) and RV Tau stars ($P > 20$ d). The main feature of RV Tau stars is alternating deep and shallow minima. However, the classification and the nature of RV Tau stars are ambiguous. Several authors suggested so-called RV Tau stars include some heterogeneous types of variables. Whilst six objects in globular clusters have been claimed to be RV Tau stars,

* E-mail: matsunaga@ioa.s.u-tokyo.ac.jp

some authors doubted this classification from both the photometric (Zsoldos 1998) and the spectroscopic point of view (Russell 1998). In this paper, we will not make a strict distinction between RV Tau stars and other T2Cs in clusters.

From previous studies of T2Cs in globular clusters, it is known that they obey period-luminosity relation (PLR) in the visible (*BVI*). Harris (1985) and McNamara (1995) claimed the slope of the PLR steepens for periods longer than about $\log P = 1$. On the other hand, Pritzl et al. (2003) did not find such a feature for the variables in the globular clusters NGC 6388 and NGC 6441. As Pritzl et al. (2003) noted, many studies of the T2Cs were based on old photographic data, and we need more investigations with modern CCD photometry. In the near-infrared, no studies have so far been reported.

Studies of variable stars in the near-infrared have become more numerous in recent times. For example, many papers have been published on the infrared properties of RR Lyr variables (e.g. Clement et al. 2001; Castellani, Caputo & Castellani 2003). RR Lyr variables also lie in the Cepheid instability strip but are fainter than T2Cs. One of the important motivations for studies of RR Lyr variables is their application as distance indicators. Whilst a larger number of investigations have been devoted to their absolute visible magnitudes, studies in the infrared have some advantages. Longmore, Fernley & Jameson (1986) and Longmore et al. (1990) discovered a well-defined PLR in the near-infrared for the first time. It was suggested that the near-infrared relation is less affected by metal abundance than the visible one, making the near-infrared one a promising distance indicator. This led to further works (Butler 2003; Dallora et al. 2004; Storm 2004; Del Principe et al. 2005). Extensive theoretical studies of the RR Lyr PLR have been also carried out (Bono et al. 2001, 2003; Catelan, Pritzl & Smith 2004; Di Criscienzo, Marconi & Caputo 2004).

In this paper, we report the result of our near-infrared observations for T2Cs in globular clusters and present their PLR in *JHK_s* filters. We also compare the PLR with that of RR Lyr variables and that of candidate T2Cs in the Large Magellanic Cloud (LMC).

2 OBSERVATIONS AND RESULTS

2.1 Observations

Data for T2Cs were obtained during our project to observe variables of various types in globular clusters. We used the Infrared Survey Facility (IRSF) 1.4 m telescope and the Simultaneous 3 Colour Infrared Imager for Unbiased Survey (SIRIUS) constructed by Nagoya University and the National Astronomical Observatory of Japan, and sited at the Sutherland station of the South African Astronomical Observatory. Images of a 7.7×7.7 arcmin² field of view are obtained simultaneously in *JHK_s*. The seeing size was typically 1.5 arcsec. For details of the IRSF and SIRIUS, see Nagashima et al. (1999) and Nagayama et al. (2003).

Our main targets in the project were red variables with long periods (100 d or more) (Matsunaga et al. 2006), so that we observed each globular cluster only once at a night. Generally, the clusters were observed once a month between April and August each year from 2002 to 2005 and on some additional occasions. The 15 or more observations obtained over this long period enable us to investigate basic properties of T2Cs. The survey targeted 145 clusters located south of about $+30^\circ$ Declination.

Table 1. The objects with periods which are different from those previously published.

Cluster	ID	P (this work)	P (previous)
NGC 5904	V84	26.87	26.42
NGC 6218	V1	15.48	15.527
NGC 6441	V6	22.47	21.365
NGC 7078	V86	16.80	17.109
NGC 7089	V6	19.36	19.30

2.2 Photometry and Variability detection

The raw data were reduced in the following way. We obtained scientific images in *JHK_s* filters for each night using pipeline software (Y Nakajima, private communication). This involved dark subtraction, flat-fielding, elimination of hot pixels, and combination of dithered images.

For each filter, one of the best images (weather condition and seeing) was selected as a reference frame among N images from the repeated observations for a globular cluster. Photometry was performed on N images with DOPHOT software (Schechter, Mateo & Saha 1993). In order to standardize the magnitudes, we compared the photometric results of the reference frames with the Two Micron All-Sky Survey (2MASS) point source catalogue (Curti et al. 2003). We found no effect of a colour term and a typical standard deviation of about ± 0.1 mag in the difference between the magnitudes in the 2MASS catalogue and ours. Colour terms were thus ignored and a constant was added to fit our instrumental magnitudes to those in the 2MASS catalogue. Note that we could use a large number of objects (say 200 or more) in these comparisons so the mean difference of our final magnitudes from the 2MASS system will be small (< 0.01 mag).

The photometric results for the remaining $N - 1$ images were compared with those of the reference frame, and we collected differences for all the detected objects. We present examples of these comparisons in Fig. 1. Variable stars stand out from the general scatter in these plots. We estimated photometric errors as a function of magnitude by taking standard deviations in boxes of size 0.25 mag or of larger size to include at least 50 objects and by smoothing the deviations. The sizes of the estimated errors ($\pm 1\sigma$) are drawn as solid curves in Fig. 1. Since some stars have larger errors due to special conditions, such as being in a crowded region, we adopted the errors from the DOPHOT software output if they exceeded the errors just discussed. We adopted a $3\text{-}\sigma$ cut to distinguish between variable and non-variable stars. Celestial coordinates of any detected variable were determined by fitting to stars in the 2MASS catalogue. The astrometrical precision is expected to be better than 0.5 arcsec in most cases.

2.3 Period Determination and the selection condition

For any object whose variation was detected in our analysis, we applied the phase dispersion minimization method in order to determine a pulsation period (Stellingwerf 1978). Even in the case of the long period stars (possible RV Tau stars), we did not discriminate between possible deep and shallow minima since the number of the minima around which we observed was not large and the differences in the infrared are small. We discuss as T2Cs in this paper, variables with the following characteristics:

- (i) the light curve shows clear periodicity of $1 < P(\text{d}) < 100$ and
- (ii) the location in the colour-magnitude diagram ($J - K_s$ versus

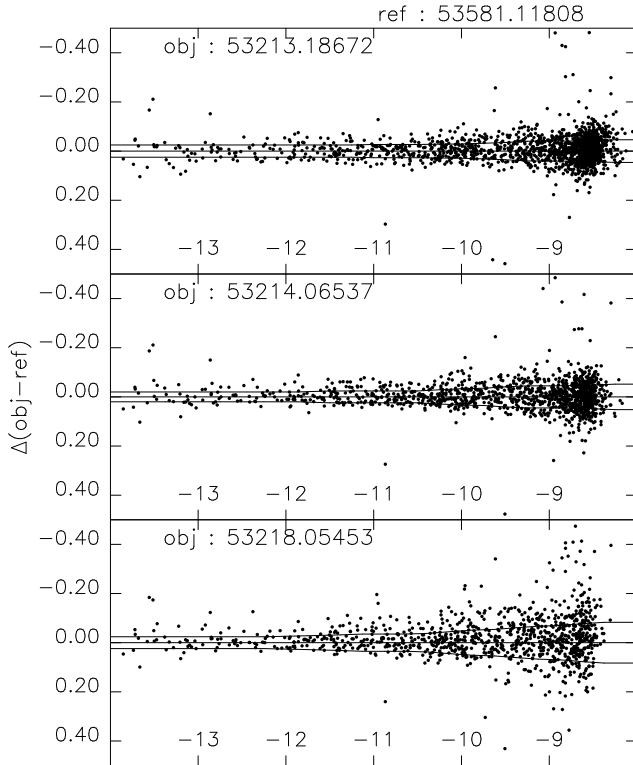


Figure 1. An example of the magnitude comparisons between the reference data (MJD= 53581.11808) and three repeated observations. These data are for the cluster NGC 104 (47 Tuc). Magnitudes on the x -axis are instrumental ones before the standardization. Solid curves indicate the size of the error in each magnitude range. See the text for details of the analysis.

K_s) is bluer than the red giant branch.

In addition, we include in the discussion known T2Cs whose variations were detected even if our data are not sufficient to determine the periods. For most of the T2Cs, periods are well determined from our data, and those obtained from the data in the three filters agree with each other. In the case of previously known T2Cs our periods are consistent with the earlier results (see Clement et al. 2001). The earlier optical periods are often based on better sampled data than ours, so that we generally adopt published periods. For five objects listed in Table 1, however, our data differ from the previous periods and we adopted our own values. All five objects have relatively long periods (W Vir stars or RV Tau stars). Clement, Hogg & Yee (1988) pointed out that some of these objects show rather random changes of the period. It is known that BL Her stars have rather systematic changes of period (Wehlau & Bohlender 1982). However, our observations were not optimized to study such effects.

2.4 Table of T2Cs

Table 2 lists 46 T2Cs obtained in our analyses. We followed the numbering system of variables by Clement et al. (2001) and the updated catalogue at their web page¹. We discovered 10 new variables, and gave them successive numbers after the ones in the Clement’s catalogue. For each variable, Table 2 lists the celestial coordinate (RA and Dec.), the period P , the date of phase zero ϕ_0 , mean magnitudes, amplitudes, and the number of observations

N_{obs} . The flag ‘n’ indicates that the object is newly discovered. The mean magnitudes are taken from the mean of maximum and minimum magnitudes and the amplitudes are defined as the minimum-to-maximum variation. Table 3 lists the individual observations. Only the first few observations are shown. The full table is given in the online version of the paper only. In this table, 99.99 is listed when we failed to obtain the magnitude. This was usually because the object was fainter than the limiting magnitude of the frame which depends on phase and the condition of the frame. We put a superscript * to the number of observations N_{obs} in Table 2 for an object with the missing measurement(s). Fig. 2 plots the light curves in K_s (against modified Julian Dates on the left-hand side and against phases folded according to the periods on the right-hand). By fitting a sine curve to each light curve in K_s , we determined phases so that the maximum light of the fitted sine curve occurs at phase zero. The value ϕ_0 listed in Table 2 is the first date of phase zero after MJD 53000 (2003 December 27).

Some of the known variables listed in Table 2 with long periods, say $P > 20$ d, were not classified as T2Cs (or RV Tau stars) in previous work. For example, NGC 6254 V1 was classified as a semi-regular type variable by Clement, Hogg & Wells (1985). It is difficult to separate the light curves of these stars from those of red variables. However, our sample is clearly defined (see previous section) and the stars we consider as T2Cs are all bluer in $J - K_s$ than the giant branch of the clusters.

Among about 80 known, or suspected, T2Cs in clusters, about half are not included in this work. Some of them were not targeted in our observations because they are located too far north (Dec. $> 30^\circ$) or too far from the cluster centre for the field of view of our camera. The others are either too faint for useful photometry or blended with a neighbouring red giant.

2.5 Chances of the contamination of field T2Cs

In Section 2.7, we show that our T2Cs define a narrow PLR. It is therefore unlikely that any of them are cluster nonmembers. However it is of interest to make some estimate of the chance of encountering a field T2C in our survey.

In the General Catalogue of Variable Stars (Kholopov 1998), there are 178 variables listed as CW (W Vir and BL Her) and 126 variables listed as RV (RV Tau). Considering their distribution over the sky, we divide them into three groups according to galactic coordinates (l, b) : the halo ($|b| > 10^\circ$), the bulge ($|l| < 10^\circ$ and $|b| < 10^\circ$), and the disc ($|l| > 10^\circ$ and $|b| < 10^\circ$). The number N and the corresponding density σ (str^{-1}) of the variables are listed in Table 4 for each group. Unfortunately, the list of field T2Cs is not based a complete, uniform, survey. Recently, Kubiak & Udalski (2003) presented the result of a T2C survey with the Optical Gravitational Lensing Experiment (OGLE) data base. They found 54 T2Cs in about 11 square degrees of the Galactic bulge. This corresponds to the density of $\sigma = 1600$ (str^{-1}), which is larger than the value listed in Table 4 by a factor of three. The solid angle of a field of view of the SIRIUS camera is 5.0×10^{-6} (str) and we observed 43 globular clusters within the bulge region. Therefore, the expected number of field T2Cs in our survey is small, less than 0.4, even in the high field density of the bulge. Since many of the clusters discussed in this paper are in much lower density environments than the bulge, the expected number of field interlopers is much less than this and can be neglected.

¹ <http://www.astro.utoronto.ca/%7Ecclement/read.html>

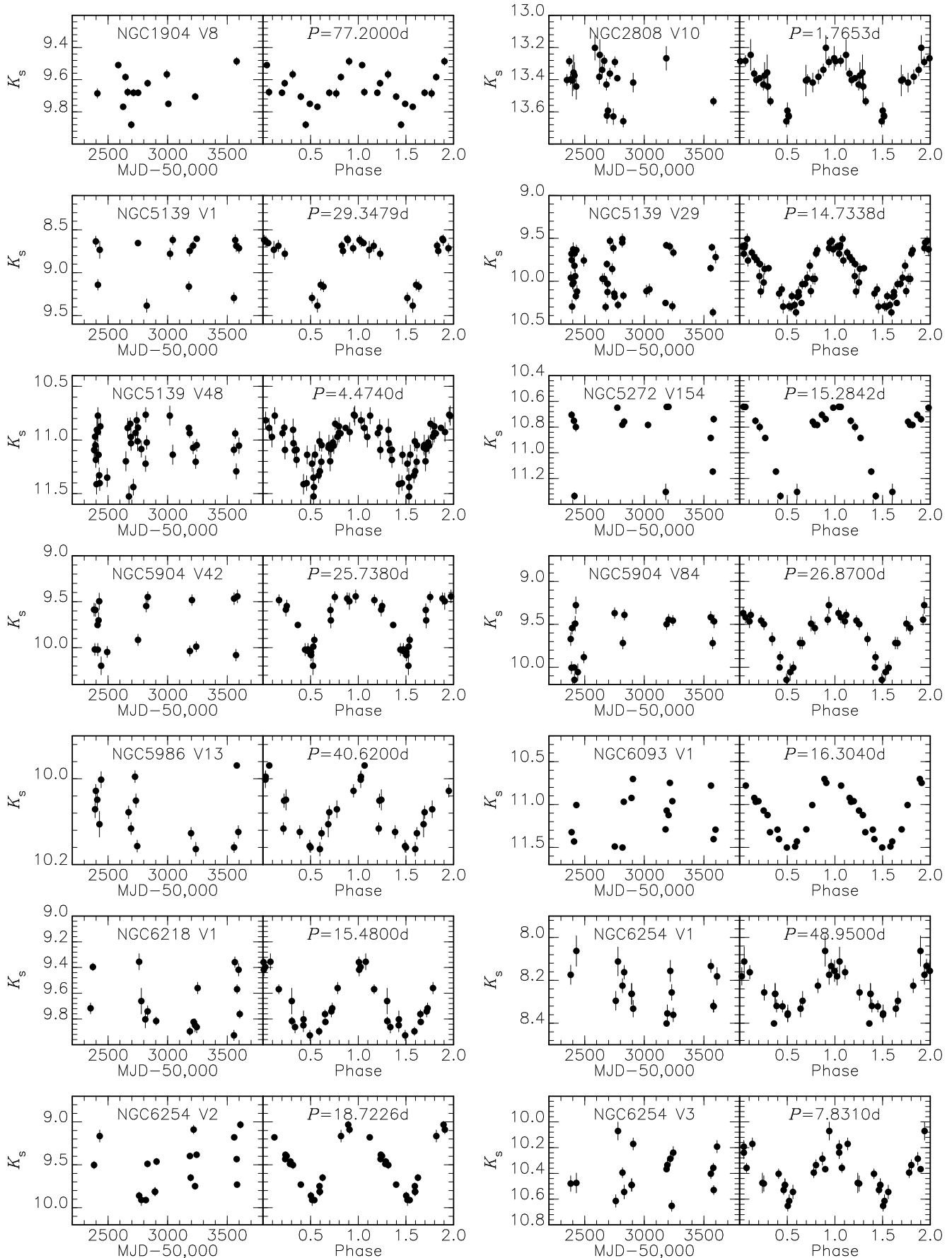


Figure 2. Light curves in K_s . Right: plotted against MJDs. Left: plotted against phases folded by the period indicated at the top of right panel.

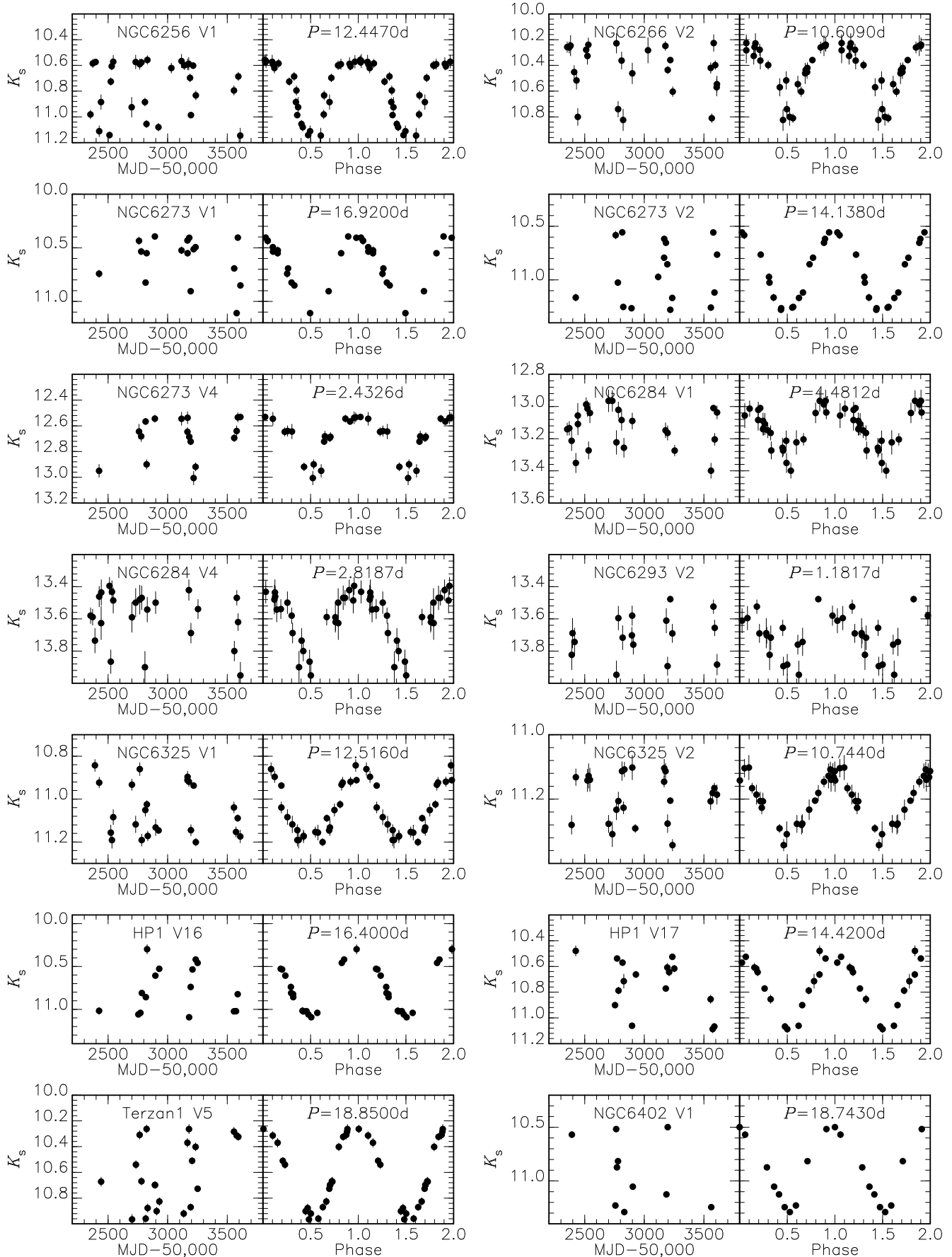


Figure 2. – continued.

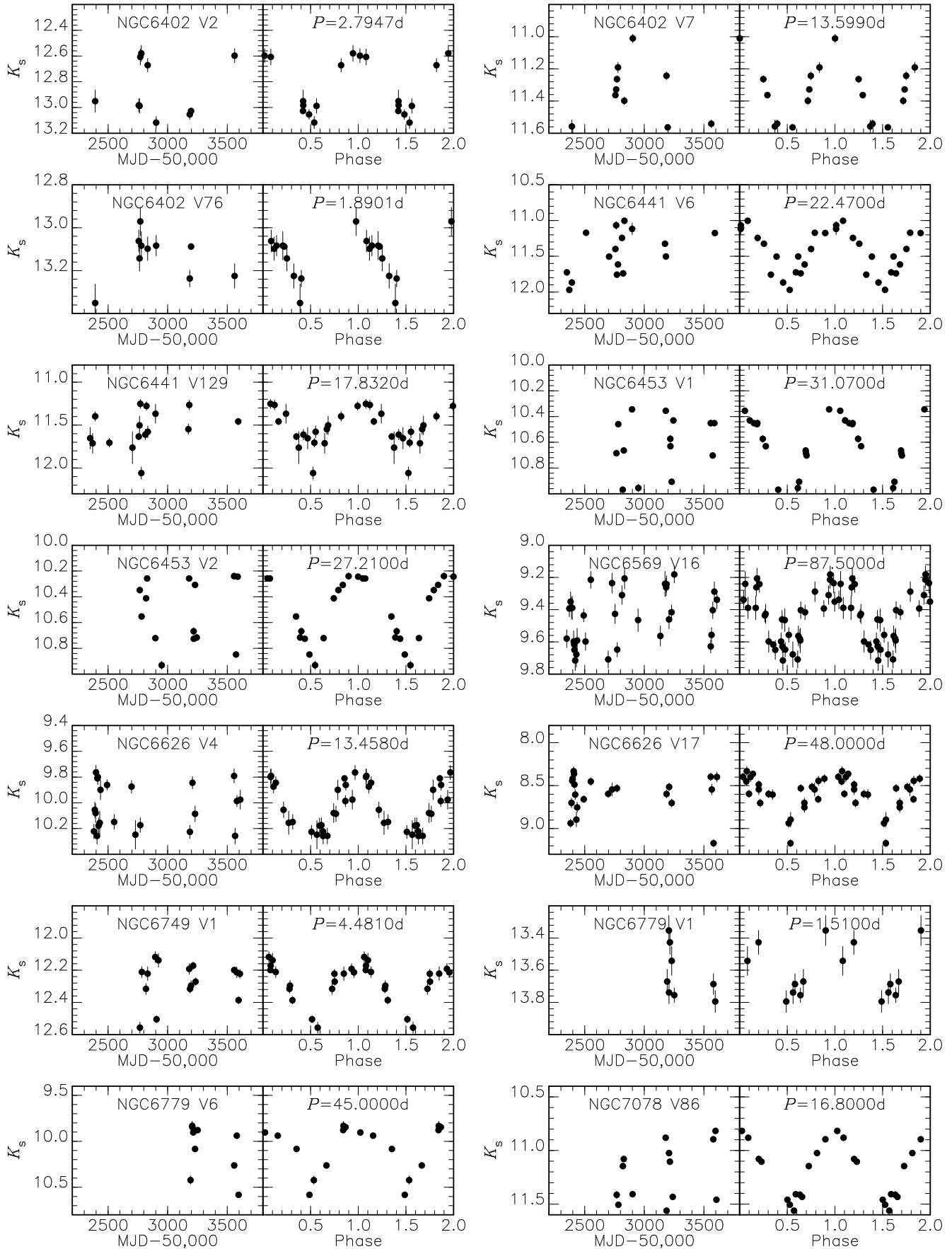


Figure 2. – continued.

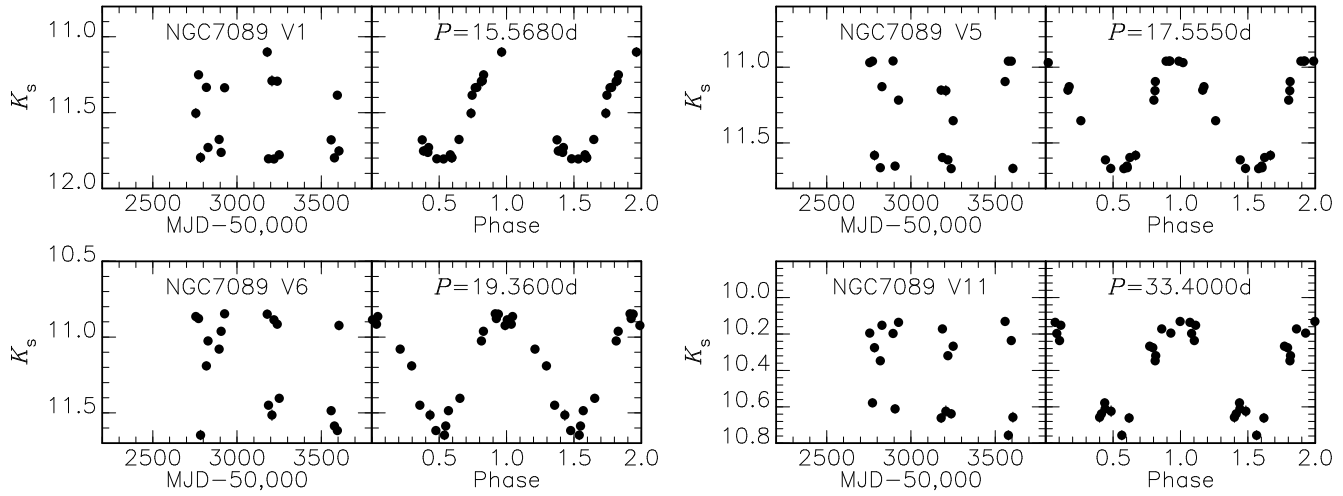


Figure 2. – continued.

Table 4. The density of T2Cs based on the General Catalogue of Variable Stars (Kholopov 1998). The regions are separated by galactic coordinate (see the text). ‘CW’ and ‘RV’ are the classified types in the catalogue for the combination of BL Her and W Vir (CW) and for RV Tau (RV).

Region	CW		RV		CW+RV	
	N	σ (str^{-1})	N	σ (str^{-1})	N	σ (str^{-1})
Halo	85	8.2	47	4.5	132	12.7
Bulge	53	438	25	207	78	645
Disk	40	19.4	54	26.2	94	45.6
All sky	178	14	126	10	304	24

2.6 Parameters for globular clusters

Now we turn to absolute magnitudes of T2Cs to combine those in different globular clusters into a period-luminosity diagram. The distance moduli we adopt are based on the magnitudes of horizontal branches of the clusters. We adopted the relation

$$M_V(\text{HB}) = 0.22[\text{Fe}/\text{H}] + 0.89 \quad (1)$$

from Gratton et al. (2003), who calibrated the relation by using the main-sequence fitting method for three clusters. Relations similar to this have also been derived by others. We adopted the values listed in the table compiled by Harris (1996), for the metal abundance $[\text{Fe}/\text{H}]$, the apparent magnitude of horizontal branch $V(\text{HB})$, and the reddening $E(B-V)$. We used the version released in 2003 February, updated in his web page², except in the case of HP 1 for which we assumed the values in the version released in 1997 May (see 2.8). For the reddening corrections, we used $R_V = 3.1$ and the following extinction law,

$$\frac{A_J}{E(B-V)} = 0.866, \quad \frac{A_H}{E(B-V)} = 0.565, \quad \frac{A_{K_s}}{E(B-V)} = 0.365 \quad (2)$$

adopted from Cardelli, Clayton & Mathis (1989).

It is known that NGC 5139 (ω Cen) has a metallicity spread and contains a population as metal rich as $[\text{Fe}/\text{H}] \sim -0.6$. However, in this cluster, a large population of horizontal branch stars

and RR Lyr stars belong to metal-poor populations and the metallicity distribution peaks at around $[\text{Fe}/\text{H}] = -1.6$ (Sillima et al. 2006). Adopting $[\text{Fe}/\text{H}] = -1.6$, the distance modulus $(m-M)_0$ is derived to be 13.62, which agrees with the value obtained from an eclipsing binary in the cluster (Thompson et al. 2001). NGC 6441 is another cluster for which we need to take special care. It has a peculiar horizontal branch and contains blue HB stars and RR Lyr stars in spite of its high metallicity (Pritzl et al. 2003). We adopted $[\text{Fe}/\text{H}] = -2.0$ for RR Lyr stars in this cluster as Pritzl et al. (2003) did, and we inserted it into equation (1). We will give more detailed discussion in Section 2.8. Our adopted metallicities, reddenings, $V(\text{HB})$ s and distance moduli are listed in Table 5.

2.7 Period-luminosity relation

The distance moduli and reddenings discussed in the last section were used to derive absolute magnitudes, and we obtained period-luminosity diagrams in three filters (Fig. 3). Linear regressions to the T2C data (filled circles) yield,

$$M_J = -2.23 (\pm 0.05)(\log P - 1.2) - 3.54 (\pm 0.03), \quad (3)$$

$$M_H = -2.34 (\pm 0.05)(\log P - 1.2) - 3.94 (\pm 0.02), \quad (4)$$

$$M_{K_s} = -2.41 (\pm 0.05)(\log P - 1.2) - 4.00 (\pm 0.02), \quad (5)$$

with residual standard deviations of 0.16, 0.15 and 0.14 mag, respectively.

Arp (1955) and Nemec, Nemec & Lutz (1994) claimed that there were fundamental-mode and first-overtone-mode pulsators forming separate parallel sequences in the T2C PLR. On the other hand, McNamara (1995) doubted the existence of any overtone pulsators. Fig. 3 shows there is no evidence for more than one mode of pulsation. As already mentioned, some papers claimed that the slope of the PL in the optical gets steeper for T2Cs at around $\log P = 1$ (Harris 1985; McNamara 1995), whilst Pritzl et al. (2003) did not find such an effect. As Fig. 3 shows there is no evidence for other than a linear relation in the near-infrared over the whole period range.

² <http://www.physics.mcmaster.ca/Globular.html>

Table 2. List of T2Cs in globular clusters. P shows a period, ϕ_0 the date of phase zero (see the text, for more detail), $\langle J \rangle$ to $\langle K \rangle$ mean magnitudes, ΔJ to ΔK amplitudes, and N_{obs} the number of observations. N_{obs} with the superscript * indicates that some of the measurements were unavailable. A flag ‘n’ indicates the object is newly discovered.

Cluster	ID	RA(J2000)	Dec(J2000)	P	ϕ_0	$\langle J \rangle$	$\langle H \rangle$	$\langle K_s \rangle$	ΔJ	ΔH	ΔK_s	N_{obs}	Flag
NGC1904	V8	05:24:11.6	-24:31:38	77.2	53046.168	10.36	9.84	9.68	0.38	0.40	0.39	13	
NGC2808	V10	09:11:56.9	-64:53:23	1.7653	53001.125	13.89	13.54	13.43	0.45	0.35	0.46	23 *	
NGC5139	V1	13:26:05.2	-47:23:43	29.3479	53013.358	9.40	9.05	8.99	0.81	0.73	0.78	15	
NGC5139	V29	13:26:27.2	-47:28:48	14.7338	53007.097	10.43	10.03	9.93	0.78	0.82	0.85	40	
NGC5139	V48	13:26:37.8	-47:30:25	4.474	53000.367	11.59	11.14	11.15	0.60	0.62	0.76	40 *	
NGC5272	V154	13:42:11.6	+28:22:14	15.2842	53003.394	11.45	11.06	10.99	0.77	0.65	0.69	14	
NGC5904	V42	15:18:24.8	+02:02:53	25.738	53020.219	10.16	9.85	9.82	0.70	0.66	0.76	18	
NGC5904	V84	15:18:36.2	+02:04:16	26.87	53018.678	10.20	9.80	9.71	1.08	0.95	0.87	18	
NGC5986	V13	15:46:00.3	-37:48:23	40.62	53009.380	10.90	10.22	10.07	0.23	0.21	0.20	15	n
NGC6093	V1	16:17:04.2	-22:58:54	16.304	53004.337	11.65	11.23	11.10	0.83	0.78	0.80	16	
NGC6218	V1	16:47:16.7	-01:57:59	15.48	53007.412	10.24	9.79	9.64	0.64	0.61	0.57	20 *	
NGC6254	V1	16:57:10.1	-04:05:36	48.95	53022.311	9.07	8.42	8.23	0.34	0.33	0.34	18 *	
NGC6254	V2	16:57:11.7	-04:04:00	18.7226	53013.656	10.05	9.61	9.47	0.90	0.94	0.88	18 *	
NGC6254	V3	16:56:56.0	-04:04:16	7.831	53007.484	11.02	10.55	10.36	0.45	0.50	0.58	18 *	
NGC6256	V1	16:59:35.0	-37:07:23	12.447	53004.719	11.86	11.15	10.85	0.73	0.60	0.59	30 *	n
NGC6266	V2	17:01:11.0	-30:07:59	10.609	53009.157	11.22	10.64	10.53	0.76	0.63	0.60	28 *	
NGC6273	V1	17:02:38.2	-26:15:12	16.92	53013.006	11.37	10.88	10.75	0.76	0.72	0.71	17	
NGC6273	V2	17:02:38.9	-26:13:57	14.138	53013.840	11.53	11.06	10.92	0.82	0.74	0.72	17	
NGC6273	V4	17:02:37.6	-26:16:32	2.4326	53000.138	13.28	12.85	12.77	0.49	0.47	0.47	17	
NGC6284	V1	17:04:26.9	-24:45:22	4.4812	53001.750	13.68	13.24	13.18	0.38	0.41	0.43	24	
NGC6284	V4	17:04:30.3	-24:46:14	2.8187	53000.533	14.15	13.71	13.67	0.64	0.52	0.56	24	
NGC6293	V2	17:09:59.8	-26:33:56	1.1817	53000.392	14.26	13.81	13.71	0.34	0.25	0.47	16	
NGC6325	V1	17:18:02.5	-23:45:45	12.516	53003.662	11.97	11.25	11.02	0.34	0.36	0.36	24 *	n
NGC6325	V2	17:17:57.8	-23:46:36	10.744	53006.200	12.14	11.43	11.22	0.24	0.26	0.24	24	n
HP1	V16	17:31:08.7	-30:00:22	16.4	53008.704	11.77	10.99	10.70	0.85	0.81	0.79	16	n
HP1	V17	17:31:05.7	-29:59:26	14.42	53004.212	11.91	11.09	10.78	0.67	0.59	0.61	16	n
Terzan1	V5	17:35:46.1	-30:29:03	18.85	53012.467	11.97	10.93	10.61	0.78	0.72	0.70	22	n
NGC6402	V1	17:37:37.4	-03:14:00	18.743	53009.449	11.63	11.10	10.89	0.85	0.80	0.79	10	
NGC6402	V2	17:37:28.6	-03:16:45	2.7947	53000.084	13.45	12.98	12.85	0.52	0.52	0.54	10	
NGC6402	V7	17:37:40.4	-03:16:21	13.599	53012.541	12.04	11.46	11.29	0.62	0.56	0.55	10	
NGC6402	V76	17:37:29.3	-03:14:45	1.8901	53001.785	13.78	13.30	13.16	0.36	0.30	0.38	10	
NGC6441	V6	17:50:15.6	-37:02:16	22.47	53010.927	12.16	11.64	11.49	0.93	0.99	0.97	16	
NGC6441	V129	17:50:12.9	-37:03:18	17.832	53001.523	12.14	11.61	11.65	0.50	0.80	0.81	16 *	
NGC6453	V1	17:50:52.1	-34:36:05	31.07	53023.985	11.51	10.85	10.66	0.70	0.62	0.62	14	n
NGC6453	V2	17:50:53.0	-34:35:09	27.21	53016.521	11.35	10.75	10.59	0.76	0.67	0.69	14	n
NGC6569	V16	18:13:37.7	-31:49:13	87.5	53081.285	10.56	9.74	9.45	0.69	0.62	0.53	34 *	
NGC6626	V4	18:24:30.1	-24:51:37	13.458	53005.162	10.78	10.18	10.01	0.68	0.52	0.49	24 *	
NGC6626	V17	18:24:35.8	-24:53:16	48	53028.399	9.55	8.95	8.75	0.84	0.84	0.84	24	
NGC6749	V1	19:05:20.0	+01:55:57	4.481	53003.020	13.38	12.62	12.34	0.38	0.44	0.44	16	n
NGC6779	V1	19:16:39.3	+30:12:17	1.51	53000.190	13.99	13.66	13.57	0.40	0.35	0.44	9 *	
NGC6779	V6	19:16:35.8	+30:11:39	45	53033.934	10.86	10.37	10.21	0.86	0.75	0.75	9	
NGC7078	V86	21:29:59.2	+12:10:07	16.8	53009.520	11.70	11.32	11.19	0.84	0.83	0.74	13	
NGC7089	V1	21:33:28.5	-00:47:55	15.568	53008.360	11.93	11.54	11.45	0.76	0.73	0.70	18	
NGC7089	V5	21:33:23.8	-00:49:13	17.555	53000.597	11.80	11.40	11.31	0.75	0.71	0.71	18	
NGC7089	V6	21:33:27.5	-00:50:00	19.36	53005.973	11.72	11.33	11.25	0.86	0.79	0.80	18	
NGC7089	V11	21:33:32.4	-00:49:06	33.4	53024.763	10.87	10.53	10.44	0.63	0.58	0.62	18	

2.8 Comments on some clusters

2.8.1 HP 1

The two T2Cs in HP 1 are of nearly the same magnitudes and periods strongly suggesting a common distance and making it unlikely that they are field stars. However, if we use the reddening in the 2003 version of the Harris catalogue [$E(B - V) = 0.74$ derived by Davidge (2000) from infrared observations of field stars], these stars lie above the PLR by amounts which depend on wavelength. This wavelength dependence is symptomatic of an incorrect reddening correction. On the other hand, using the reddening from the 1997 version of the Harris catalogue places the star on the PLR at

all wavelengths. This latter reddening ($E(B - V) = 1.19$) was obtained by Ortolani, Bica & Barbuy (1997) from a comparison of the $(V - I)$ colour of the RGB with that of NGC 6752. Other authors have also found reddenings larger than that derived by Davidge (i.e. $E(B - V) = 1.44$, Armandroff & Zinn 1988; 1.88, Minniti 1995). We have therefore used the Ortolani value of the reddening.

2.8.2 NGC 6441

Despite the relatively high metallicity usually adopted for NGC 6441 ($[\text{Fe}/\text{H}] = -0.53$; Harris 1996), Rich et al. (1997) discovered it to have a blue horizontal branch as does the related

Table 3. The first 15 lines in the released table of light variation. This is a sample of the full version (862 lines), which will be available in the online version of this journal. Each line lists the data of each observation: MJD (modified Julian Date), phase (zero for the maxima), magnitudes (JHK_s), and errors (E_J , E_H and E_{K_s}).

Cluster	ID	MJD	Phase	J	E_J	H	E_H	K_s	E_{K_s}
NGC1904	V8	52410.6926	0.688	10.38	0.02	9.86	0.02	9.69	0.03
NGC1904	V8	52586.1033	0.960	10.21	0.03	9.67	0.02	9.51	0.02
NGC1904	V8	52627.0778	0.491	10.45	0.03	9.91	0.02	9.77	0.01
NGC1904	V8	52646.0534	0.736	10.25	0.03	9.77	0.02	9.58	0.02
NGC1904	V8	52665.0233	0.982	10.36	0.02	9.86	0.03	9.68	0.02
NGC1904	V8	52694.8237	0.368	10.55	0.03	10.04	0.02	9.88	0.02
NGC1904	V8	52713.8921	0.615	10.34	0.02	9.86	0.02	9.68	0.02
NGC1904	V8	52752.7671	0.119	10.38	0.03	9.87	0.02	9.68	0.02
NGC1904	V8	52832.2021	0.148	10.34	0.02	9.79	0.02	9.62	0.02
NGC1904	V8	52993.0750	0.231	10.27	0.02	9.75	0.01	9.57	0.03
NGC1904	V8	53006.9818	0.412	10.46	0.02	9.93	0.01	9.75	0.01
NGC1904	V8	53231.1906	0.316	10.40	0.03	9.88	0.01	9.71	0.02
NGC1904	V8	53579.1520	0.823	10.18	0.02	9.64	0.02	9.49	0.03
NGC2808	V10	52351.8047	0.702	13.87	0.03	13.48	0.03	13.40	0.04
NGC2808	V10	52370.9252	0.533	13.78	0.04	13.36	0.04	13.29	0.03

Table 5. Parameters for globular clusters. The metallicity $[\text{Fe}/\text{H}]$, the colour excess $E(B - V)$, and the magnitude of the horizontal branch $V(\text{HB})$ were adopted from Harris (1996). The distance modulus $(m - M)_0$ was estimated from equation (1), except for NGC 6441 (see the text).

Cluster	$[\text{Fe}/\text{H}]$	$E(B - V)$	$V(\text{HB})$	$(m - M)_0$
NGC 1904	-1.57	0.01	16.15	15.57
NGC 2808	-1.15	0.22	16.22	14.90
NGC 5139	-1.6	0.12	14.53	13.62
NGC 5272	-1.57	0.01	15.68	15.10
NGC 5904	-1.27	0.03	15.07	14.37
NGC 5986	-1.58	0.28	16.52	15.11
NGC 6093	-1.75	0.18	16.10	15.04
NGC 6218	-1.48	0.19	14.60	13.45
NGC 6254	-1.52	0.28	14.65	13.23
NGC 6256	-0.70	1.03	18.50	14.57
NGC 6266	-1.29	0.47	16.25	14.19
NGC 6273	-1.68	0.41	16.50	14.71
NGC 6284	-1.32	0.28	17.40	15.93
NGC 6293	-1.92	0.41	16.50	14.76
NGC 6325	-1.17	0.89	17.90	14.51
NGC 6402	-1.39	0.60	17.30	14.86
HP 1	-1.50	1.19	18.60	14.36
Terzan 1	-1.30	2.28	21.40	13.73
NGC 6441	-0.53	0.47	17.51	15.60
NGC 6453	-1.53	0.66	17.53	14.93
NGC 6569	-0.86	0.55	17.52	15.11
NGC 6626	-1.45	0.40	15.55	13.74
NGC 6749	-1.60	1.50	19.70	14.51
NGC 6779	-1.94	0.20	16.16	15.08
NGC 7078	-2.26	0.10	15.83	15.13
NGC 7089	-1.62	0.06	16.05	15.33

cluster NGC 6388. These clusters have many RR Lyr variables (Layden et al. 1999; Pritzl et al. 2003, and references therein), and these RR Lyr stars resemble those in Oosterhoff II clusters (metal poor) rather than those in Oosterhoff I ones (relatively metal rich). Nevertheless, Clementini et al. (2005) have recently reported that RR Lyr stars in NGC 6441 are not of low metallicity. Pritzl et al. (2000) suggested that they comprise a new Oosterhoff group and they found circumstantial evidence that they may be at least as

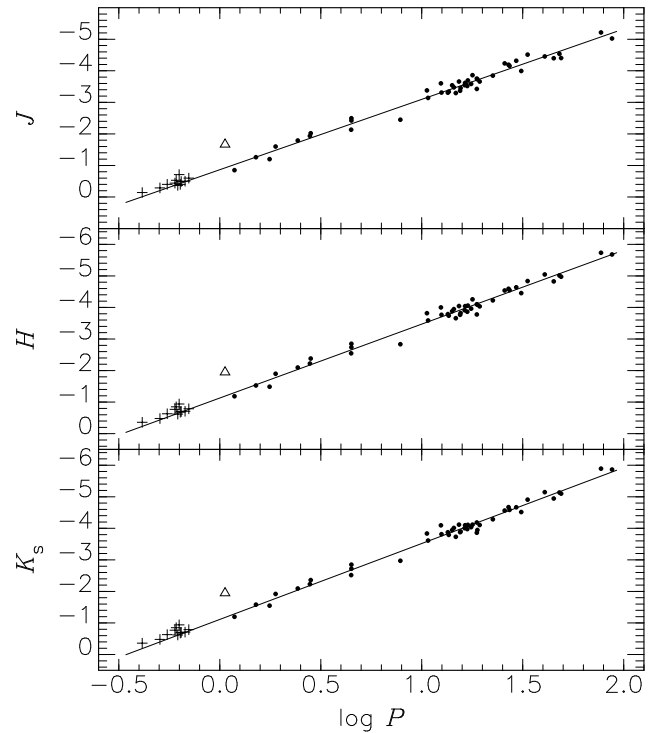


Figure 3. Period-luminosity relation in JHK_s filters for type II Cepheids (filled circles). Linear regressions (to filled circles) are shown as solid lines. The data for RR Lyr variables in NGC 6341 are also plotted as plus symbols taken from Del Principe et al. (2005). The triangle at $\log P = 0.026$ is the data for NGC 6341 V7. See the discussion in Section 3.2 for RR Lyr variables and NGC 6341 V7.

bright as those in the very metal-poor clusters. In view of these results we have followed (Pritzl et al. 2003) and used an absolute magnitude for the HB of this cluster equivalent to that of one with $[\text{Fe}/\text{H}] = -2.0$. There is very little doubt that the T2Cs belong to NGC 6441 since there are still four more T2Cs observed optically, but in the crowded cluster centre not observed by us, besides the two discussed here. They have (optical) magnitudes consistent with the ones we have studied (Pritzl et al. 2003). In so much as

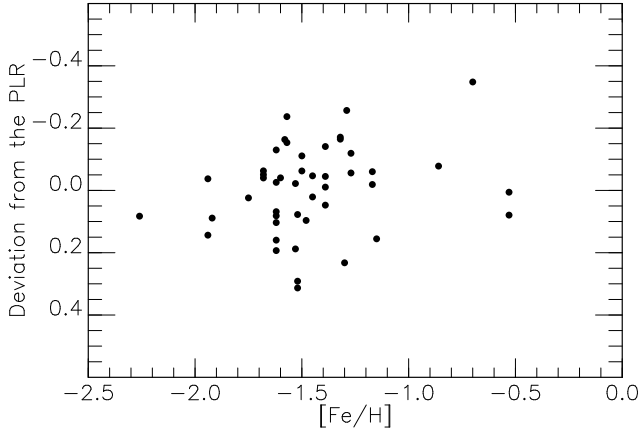


Figure 4. The relation between the metallicity and the deviation from the PLR in K_s .

the T2Cs in NGC 6441 fall on our PL relation at our adopted distance, they support the high luminosities for the RR Lyr variables as discussed by Pritzl et al. (2000).

3 DISCUSSION

3.1 Metallicity effect on the PLR

First, we discuss the metallicity effect on the zero-point of the PLR, by comparing deviations from the PLR (3) – (5) with the metallicity for each object. We simply adopted the metallicity of the globular cluster, in which a T2C is found, as the metallicity of the T2C. The relation in the K_s filter is shown in Fig. 4. The distance moduli we used equation (1) have of course a metallicity dependence by themselves. A linear regression for the data in Fig. 4 has a slope of $-0.10(\pm 0.06)$ which is hardly significant. It would be reduced to -0.02 if we adopted the slope of 0.30 for equation (1) derived earlier by Sandage (1993). Note that adopting the latter slope makes negligible difference (less than 1 percent) to our PLR slopes.

3.2 Extension of the PLR to RR Lyr region

We found that RR Lyr variables also obey the PLR (3) – (5). Plus symbols in Fig. 3 indicate RR Lyr variables in NGC 6341 (M 92) taken from Del Principe et al. (2005). We adopted a distance modulus of 14.65 mag obtained in the same manner as for other clusters (equation 1). This is the only cluster with RR Lyr observations at all three wavelengths. A comparison can be made at K_s for a number of other clusters. As shown in Fig. 5, both the slope and the zero-point of the PLR agree satisfactorily with that of the RR Lyr variables in all cases. The data for the RR Lyr variables are from (Longmore et al. 1990), (Butler 2003), (Storm 2004), and (Del Principe et al. 2005). We averaged the results for the eight globular clusters in Longmore et al. (1990). Although their magnitudes are K (not K_s) in various photometric system, the differences are negligible (less than 0.01 mag; see Carpenter 2001, for example). Theoretical studies also provided sufficiently close PLRs. For example, the slope in Bono et al. (2001) was -2.07 and that in Catelan et al. (2004) was -2.35 . These works showed that there is a small metallicity dependence of the zero-point ($\sim 0.17 \log Z$ in K), but the effect is not clear in the observational results and must be small (Longmore et al. (1990) derived the metallicity-dependent term as $0.04[\text{Fe}/\text{H}]$). These results carry the implication that stars

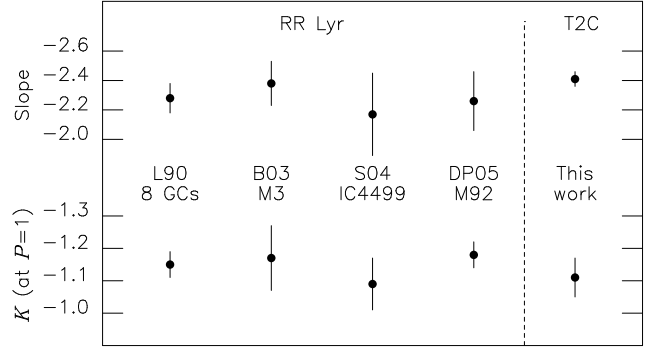


Figure 5. Comparison of the slope and the zero-point of the PLR of T2Cs (this work) and those of RR Lyr variables in references. L90 shows the result of Longmore et al. (1990), B03 Butler (2003), S04 Storm (2004) and DP05 Del Principe et al. (2005).

with the same age and probably the same mass within the instability strip obey the same PLR. We will discuss this in next section.

Some comments should be provided about NGC 6341 V7 (Del Principe et al. 2005), which has a period of $\log P = 0.0259$ and is deviant from the PLR (the triangle in Fig. 3). Unfortunately, NGC 6341 lies too north to be observed by us. Kopacki (2001) reported that this star is a BL Her star, but it is apparently brighter than expected from our PLR. Although we need to confirm its membership, the location of NGC6341 in the halo indicates that this star belongs to the cluster (see Section 2.5). In that case, this star may be the second anomalous Cepheid in globular clusters after NGC 5466 V19. An anomalous Cepheid is a more massive variable with $0.3 < P(d) < 2$ and is brighter than RR Lyr variables by about one magnitude (Zinn & Dahn 1976; Cox & Proffitt 1988). This star needs further investigation, including a confirmation of cluster membership.

3.3 Reproduction of the PLR

Here, we discuss the PLR by using the $P\sqrt{\rho} = Q$ relation. The relation can be written as

$$M_{\text{bol}} = -3.33 \log P - 1.67 \log M - 10 \log T_{\text{eff}} + M_{\text{bol},\odot} + 10 \log T_{\text{eff},\odot} + 3.33 \log Q, \quad (6)$$

where M is the mass in units of the solar mass, and T_{eff} the effective temperature (e.g. McNamara 1995). Two linear relations,

$$\log T_{\text{eff}} = -0.058 \log P + 3.81, \quad (7)$$

$$\log Q = 0.24 \log P - 1.39, \quad (8)$$

are adopted from McNamara & Pyne (1994) to derive the PLR. We express the bolometric correction as

$$M_{\text{bol}} - M_{\lambda} = \alpha_{\lambda} \log T_{\text{eff}} + \beta_{\lambda}. \quad (9)$$

Using these relations, eq (6) can be expressed in the form,

$$M_{\lambda} = -(1.95 - 0.058\alpha_{\lambda})(\log P - 1.2) - 1.67 \log M - (2.70 + 3.74\alpha_{\lambda} + \beta_{\lambda}) \quad (10)$$

with the constants of $M_{\text{bol},\odot} = 4.75$ and $T_{\text{eff},\odot} = 5780\text{K}$. We define μ_{λ} and η_{λ} as the dependence on the period ($dM_{\lambda}/d \log P$) and the zero-point of the relation at $\log P = 1.2$, respectively [i.e. $M_{\lambda} = \mu_{\lambda}(\log P - 1.2) + \eta_{\lambda}$]. If the mass term ($\log M$) has no

dependence on the period, μ_λ equals to $-(1.95 - 0.058\alpha_\lambda)$. However, Bono, Caputo & Santolamazza (1997) predicted that the mass of T2Cs varies from $0.59M_\odot$ to $0.52M_\odot$, decreasing with increasing period from 1 to 10 d. This period dependence increases μ_λ by 0.08 compared with the case of the constant mass.

We obtained α_λ and β_λ in Table 6 from the model atmospheres listed in table 1 of Bessell, Castelli & Plez (1998). They listed both the models with overshooting (table 1) and those without overshooting (table 2), but the difference between the two sets has negligible effect on our results (up to 0.03 mag). Whilst these models are computed with the solar metallicity, Sandage, Bell & Tripicco (1999) computed model atmospheres for Cepheids between $[\text{Fe}/\text{H}] = 0.0$ and -1.7 . Their results show that the slopes of the $\log T_{\text{eff}}$ -bolometric correction relation (equation 9) are within the uncertainty of our adopted values, and the zero-points get slightly smaller for the lower metallicity (about 0.1-mag difference between $[\text{Fe}/\text{H}] = 0.0$ and -1.7). In JHK_s filters we would expect any effect of metallicity on equation (9) to be less than in V and I .

The third and fourth columns in Table 6 show the predicted slope μ_λ and zero-point η_λ in case of constant mass. They are approximately consistent with the counterparts obtained from the observational data (the fifth and sixth columns). The observational values in V and I filters are taken from Pritzl et al. (2003) and those in JHK_s filters are obtained by us. Fig. 6 shows the relation between α_λ and μ_λ . The solid line shows the case of constant mass, and the broken one shows the one shifted by 0.08 for the mass-dependent case. The observational values (filled circles) favour the constant mass model at least in our own data (JHK_s). In V , the slope expected from equation (10) is steeper than the observational value. A linear fit to the bolometric correction (equation 9) is not very good in V , since a quadratic term is no longer small unlike the case of JHK_s . The value of α_V in equation (9) can range from 0 to 4 between the extreme values of $\log T_{\text{eff}}$, 3.85 and 3.70. If we adopt a quadratic relation instead of equation (9), the PLR also become quadratic and the slope of a linear fit to the entire period range is about -1.7 in V , which is close to the observational value (-1.64). Since our discussion is based on very simple scheme, more detailed work on both the theoretical and observational side is desirable.

It is worth noting that T2Cs and RR Lyr variables may be unique in that they comprise a group of variables with almost a constant mass obeying PLRs. For instance in the cases of classical Cepheids and Mira variables the mass increases with increasing period. It is therefore interesting that our PLRs can be reproduced by the simple scheme with a constant mass and no need to adopt a mass-luminosity relation.

3.4 Comparison with T2Cs in the LMC

Alcock et al. (1998) reported 33 candidate T2Cs with $8 < P(\text{d}) < 100$ based on the Massive Compact Halo Object (MACHO) data base in the LMC. We searched for their near-infrared magnitudes in the 2MASS point-source catalog (Curti et al. 2003), and found 27 matches among 33 objects (Table 7). Fig. 7 shows the PLR in JHK_s for the T2Cs in the LMC (crosses). Also plotted (filled circles) are the T2Cs in globular clusters. The absolute magnitudes for the LMC objects were obtained with an assumed distance modulus of 18.50 mag. There are some uncertainties of about ± 0.3 mag in using the 2MASS data because they are based on single-epoch observations. However, it seems rather clear that longer period LMC variables ($P > 40\text{d}$) are brighter than the counterparts in globular clusters. The LMC variables at shorter periods fit the PLR of globular clusters within the uncertainties. This feature is also seen in the

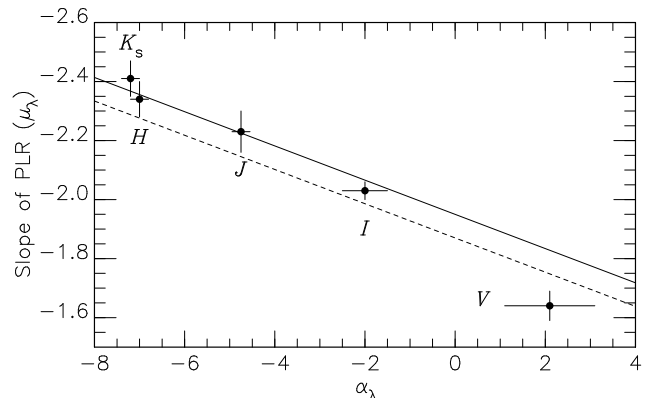


Figure 6. The relation between the adopted bolometric correction (α_λ) and the slope of the PLR (μ_λ). The solid line indicates the relation according to equation (10) in case of the constant mass, and the broken one is the one shifted by 0.08 considering the mass dependency mentioned in the text. Filled circles show the observational results.

$\log P$ - V diagram (fig. 9) in Pritzl et al. (2003), but their conclusion is somewhat uncertain because they do not have their own data for the cluster variables with $P > 40$ d [compare the panels (a) and (d) of their fig. 9].

A mass difference could be one of the reasons for the LMC RV Tau stars being about one magnitude brighter than the globular cluster PLRs. Massive variables are expected to be brighter according to equation (10). A difference of about 1 mag corresponds to an increase in mass by a factor of about 4. Considering that the masses of the globular cluster variables are about $0.5 - 0.6 M_\odot$, this would lead to a mass larger than the Chandrasekhar limit for the LMC RV Tau stars. This is too large if these variables are post-AGB stars which have already gone through their major mass-loss phase (e.g. Jura 1986; Pollard & Lloyd Evans 1999). In that case some other parameter is necessary to explain the difference in absolute magnitude.

Fig. 8 shows a colour-colour diagram for the variables with $P > 20$ d in globular clusters (filled circles) and the LMC (crosses) and also for the galactic field RV Tau stars (triangles) taken from Lloyd Evans (1985). The colours of our cluster objects and the LMC objects were corrected for reddenings, while those of the galactic field objects were not because Lloyd Evans (1985) did not give any estimate of the reddenings. More than half of the galactic field objects have the galactic latitudes of $|b| > 5^\circ$ so that the reddening effect on the colour is expected to be not large ($E(H - K) < 0.1$). The large excesses of the $K - L$ colours reported by Lloyd Evans (1985), which should be smaller than $E(H - K)$ in the case of interstellar reddening, also support that the objects are intrinsically red. In Fig. 8, the globular cluster sample occupies a rather limited region whilst many of the LMC and the local stars spread to redder $H - K_s$ colour. As mentioned in Section 1, the classification of the longer period variables ($P > 20$ d) in globular clusters as RV Tau stars is unclear. One of the characteristics often seen in RV Tau stars is an infrared excess caused by their circumstellar dust shells (Jura 1986). The only globular cluster RV Tau star which has been claimed to have an infrared excess is NGC 6626 V17. Nook & Cardelli (1989) found an excess at $10 \mu\text{m}$ in this star. However, NGC 6626 V17 which has $(H - K)_0 = 0.12$ and $(J - H)_0 = 0.48$ lies with the other cluster stars in Fig. 8, and it also lies on our PLRs. We conclude that RV Tau stars in the LMC belong to a different family of variables from the T2Cs of the same

Table 6. The relation between the adopted bolometric correction ($\alpha_\lambda, \beta_\lambda$) and the PLR (slope μ_λ and zero-point η_λ). Observational values for JHK_s are from the present paper, and those for V and I filters are from Pritzl et al. (2003).

Filter	α_λ	β_λ	Equation (10)		Observation	
			μ_λ	η_λ	μ_λ	η_λ
V	$+2.1 \pm 1.0$	-7.06	-1.85	-1.94	-1.64 ± 0.05	-1.92
I	-2.0 ± 0.5	9.11	-2.08	-2.77	-2.03 ± 0.03	-2.80
J	-4.75 ± 0.1	19.40	-2.23	-3.34	-2.23 ± 0.07	-3.54
H	-7.0 ± 0.1	27.66	-2.36	-3.75	-2.34 ± 0.06	-3.94
K_s	-7.2 ± 0.1	28.47	-2.37	-3.81	-2.41 ± 0.06	-4.00

Table 7. 2MASS magnitudes for candidate T2Cs in the LMC. Star IDs are from Alcock et al. (1998).

Star ID	P	J	H	K_s
1.3812.61	9.387	15.453	14.970	15.222
10.4040.38	9.622	14.635	14.153	13.998
80.6469.135	10.509	15.749	15.483	15.125
80.6590.137	11.442	15.347	14.824	14.771
3.7332.39	12.704	15.868	15.380	15.178
80.6475.2289	13.925	15.003	14.611	14.373
81.9006.64	14.337	15.053	14.647	14.469
47.2611.589	14.469	15.793	15.326	15.183
19.4425.231	14.752	14.963	14.899	14.473
2.5877.58	14.855	15.857	15.389	15.033
1.3808.112	14.906	15.209	14.758	14.703
14.8983.1894	15.391	14.988	14.500	14.526
2.5025.39	16.602	14.723	14.369	14.368
9.5117.58	16.747	14.697	14.394	14.199
10.3680.18	17.127	14.836	14.424	14.254
78.6338.24	17.560	14.354	14.120	14.002
2.5026.30	21.486	14.571	14.136	13.984
78.6698.38	24.848	14.281	13.823	13.463
77.7069.213	24.935	15.364	14.676	14.457
82.8041.17	26.594	14.584	14.088	13.877
19.6394.19	31.716	14.011	13.641	13.356
78.5856.2363	41.118	13.668	13.250	13.179
81.8520.15	42.079	13.547	13.251	13.166
82.8405.15	46.542	13.114	12.884	12.569
81.9728.14	47.019	13.201	12.635	12.098
79.5501.13	48.539	13.089	12.635	12.093
47.2496.8	56.224	13.124	12.709	12.512

periods in globular clusters. Whether they define a PLR is not clear.

4 SUMMARY

We have shown from our near-infrared observations of T2Cs in globular clusters that they define linear PLR at JHK_s with little scatter. There is no evidence for a change of the slope at around $\log P = 1$, such as was suggested at V in some early papers. An extrapolation of our infrared relation is shown to fit globular cluster RR Lyr variables. Both the slopes and the zero-points of the infrared PLRs can be successfully reproduced by a simple application of the pulsation equation at constant mass. The T2Cs and the RR Lyr variables in clusters therefore seem to form an interesting family of stars all with closely the same mass and showing a common PLR.

2MASS JHK_s magnitudes for W Vir stars and RV Tau stars

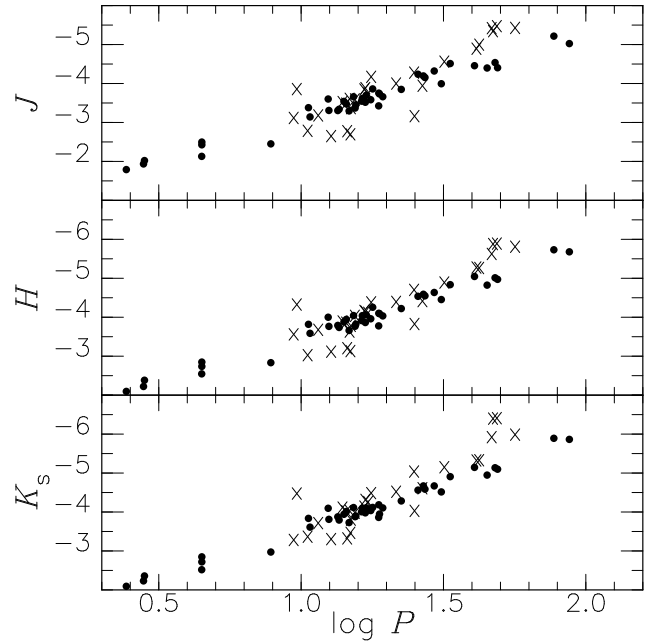


Figure 7. The PLR for the globular cluster sample (filled circles) and the LMC candidates (crosses).

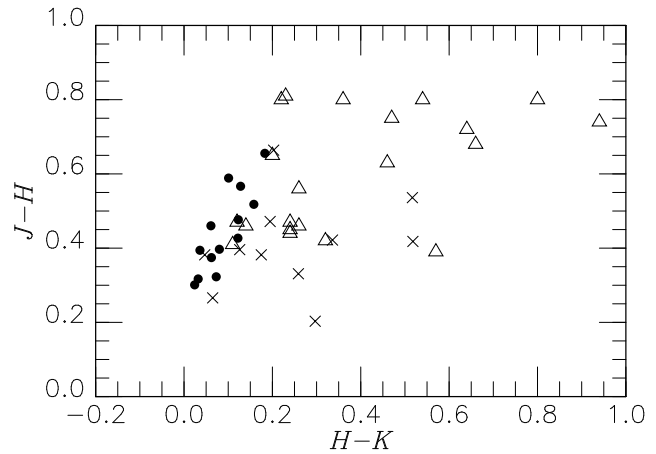


Figure 8. A colour-colour diagram for variables with $P > 20$ d: filled circles for globular cluster stars, crosses for the LMC stars from Alcock et al. (1998) and triangles for galactic field stars (Lloyd Evans 1985). The colours of the globular cluster stars and the LMC stars were corrected for the rednings, while those of the galactic field stars were not (see the text).

in the Large Magellanic Clouds show that, within the uncertainties, W Vir stars with $P < 20$ (d) obey the same PLR as those for the globular cluster T2Cs. However, RV Tau stars with $P > 40$ (d) are brighter than variables of the same periods in globular clusters. The reason for this is unclear, but the distribution in the $(H - K_s)$ - $(J - H)$ diagram also shows differences between the two groups. RV Tau stars in the LMC are generally redder than those in globular clusters as are RV Tau stars in the galactic field.

ACKNOWLEDGMENTS

We thank Dr Patricia Whitelock for her help on a part of observation. The IRSF/SIRIUS project was initiated and supported by Nagoya University, the National Astronomical Observatory of Japan and the University of Tokyo in collaboration with the South African Astronomical Observatory under a financial support of grant-in-aid for Scientific Research on Priority Area (A) No. 10147207 and 10147214 and the grant-in-aid for Scientific Research (C) No. 15540231 of the Ministry of Education, Culture, Sports, Science and Technology of Japan. One of the authors (NM) is financially supported by the Japan Society for the Promotion of Science (JSPS) through JSPS research fellowships for young scientists.

REFERENCES

- Alcock C. et al., 1998, AJ, 115, 1921
 Armandroff T. E., Zinn R., 1988, AJ, 96, 92
 Arp H. C., 1955, AJ, 60, 1
 Bessell M. S., Castelli F., Plez B., 1998, A&A, 333, 231
 Bono G., Caputo F., Castellani V., Marconi M., Storm J., 2001, MNRAS, 326, 1183
 Bono G., Caputo F., Castellani V., Marconi M., Storm J., Degl'Innocenti S., 2003, MNRAS, 344, 1097
 Bono G., Caputo F., Santolamazza P., 1997, A&A, 317, 171
 Butler D. J., 2003, A&A, 405, 981
 Cardelli J. A., Clayton G. C., Mathis J. S., 1989, ApJ, 345, 245
 Carpenter J. M., 2001, AJ, 121, 2851
 Castellani M., Caputo F., Castellani V., 2003, A&A, 410, 871
 Catelan M., Pritzl B. J., Smith H. A., 2004, ApJS, 154, 633
 Clement C. M., Hogg H. S., Wells T. R., 1985, AJ, 90, 1238
 Clement C. M., Hogg H. S., Yee A., 1988, AJ, 96, 1642
 Clement C. M. et al., 2001, AJ, 122, 2587
 Clementini G., Gratton R. G., Bragaglia A., Ripepi V., Fiorenzano A. F. M., Held E. V., Carretta E., 2005, ApJ, 630, L145
 Cox A. N., Proffitt C. R., 1988, ApJ, 324, 1042
 Curti R. M. et al., 2003, Explanatory Supplement to the 2MASS All Sky Data Release. Caltech, Pasadena, p. 1
 Dall'Ora M. et al., 2004, ApJ, 610, 269
 Davidge T. J., 2000, ApJS, 126, 105
 Del Principe M., Piersimoni A. M., Bono G., Di Paola A., Dolci M., Marconi M., 2005, AJ, 129, 2714
 Di Criscienzo M., Marconi M., Caputo F., 2004, ApJ, 612, 1092
 Gratton R. G., Bragaglia A., Carretta E., Clementini G., Desidera S., Grundahl F., Lucatello S., 2003, A&A, 408, 529
 Harris H. C., 1985, in Madore B. F. ed., Cepheids: Theory & Observations. Cambridge University Press, Cambridge, p. 232
 Harris W. E., 1996, AJ, 112, 1487
 Jura M., 1986, ApJ, 309, 732
 Kholopov P. N. et al., 1998, Combined General Catalogue of Variable Stars, 4.1 edn. (CDS II/214A)
 Kopacki G., 2001, A&A, 369, 862
 Kubiak M., Udalski A., 2003, Acta Astron., 53, 117
 Layden A. C., Ritter L. A., Welch D. L., Webb T. M. A., 1999, AJ, 117, 1313
 Lloyd Evans T., 1985, MNRAS, 217, 493
 Longmore A. J., Dixon R., Skillen I., Jameson R. F., Fernley J. A., 1990, MNRAS, 247, 684
 Longmore A. J., Fernley J. A., Jameson R. F., 1986, MNRAS, 220, 279
 McNamara D. H., Pyne M. D., 1994, PASP, 106, 472
 McNamara D. H., 1995, AJ, 109, 2134
 Matsunaga, N., Nakada Y., Tanabé T., Fukushi H., Ita Y., 2006, Mem. Soc. Astron. Ital., 77, 63
 Minniti D., 1995, A&A, 303, 468
 Nagashima C. et al., 1999, in Nakamoto T., ed., Star Formation 1999, Nobeyama Radio Observatory, Nobeyama, p. 397
 Nagayama T. et al., 2003, Proc. SPIE, 4841, 459
 Nemec J. M., Nemec A. F. L., Lutz T. E., 1994, AJ, 108, 222
 Nook M. A., Cardelli J. A., 1989, ApJ, 346, L29
 Ortolani S., Bica E., Barbuy B., 1997, MNRAS, 284, 692
 Pollard K. R., Lloyd Evans T., 1999, Int. Astron. Union Symp., 191, 459
 Pritzl B. J., Smith H. A., Catelan M., Sweigart A. V., 2000, ApJ, 530, L41
 Pritzl B. J., Smith H. A., Catelan M., Sweigart A. V., 2002, AJ, 124, 949
 Pritzl B. J., Smith H. A., Stetson P. B., Catelan M., Sweigart A. V., Layden A. C., Rich R. M., 2003, AJ, 126, 1381
 Rich M. R. et al., 1997, ApJ, 484, L25
 Russell S. C., 1998, Publ. Astron. Soc. Aust., 15, 189
 Sandage A., 1993, AJ, 106, 703
 Sandage A., Bell R. A., Tripicco M. J., 1999, ApJ, 522, 250
 Schechter P. L., Mateo M., Saha A., 1993, PASP, 105, 1342
 Sollima A., Borissova J., Catelan M., Smith H. A., Minniti D., Cacciari C., Ferraro F. R., 2006, ApJ, 640, L43
 Stellingwerf R. F., 1978, ApJ, 224, 953
 Storm J., 2004, A&A, 415, 987
 Thompson I. B., Kaluzny J., Pych W., Burley G., Krzeminski W., Paczyński B., Persson S. E., Preston G. W., 2001, AJ, 121, 3089
 Wallerstein G., 2002, PASP, 114, 689
 Wehlau A., Bohlender D., 1982, AJ, 87, 780
 Zinn R., Dahn C. C., 1976, AJ, 81, 527
 Zsoldos E., 1998, Acta Astron., 48, 775